

THE BEHAVIOR OF Cr DURING METAMORPHISM OF CARBONATE ROCKS FROM THE NEVADO-FILÁBRIDE COMPLEX, BETIC CORDILLERAS, SPAIN

VICENTE LÓPEZ SÁNCHEZ-VIZCAÍNO

*Departamento de Mineralogía y Petrología, Instituto Andaluz de Geología Mediterránea (CSIC),
Facultad de Ciencias, Avda. Fuentenueva s/n, 18002 Granada, Spain*

GERHARD FRANZ

Fachgebiet Petrologie, Technische Universität Berlin, Strasse des 17 Juni 135, 10623 Berlin, Germany

MARÍA TERESA GÓMEZ-PUGNAIRE

*Departamento de Mineralogía y Petrología, Instituto Andaluz de Geología Mediterránea (CSIC),
Facultad de Ciencias, Avda. Fuentenueva s/n, 18002 Granada, Spain*

ABSTRACT

Some metacarbonate rocks from the Nevado-Filábride Complex (Betic Cordilleras, southern Spain) contain unusual quantities of Cr-rich minerals. These occur in very thin layers concentrated in beds a few meters thick, interbedded with other lithologies (metapelites and metacarbonates) devoid of chromium. Cr₂O₃ contents reported here reach values (in wt.%) of 5.74 in epidote, 5.09 in phengitic muscovite, 1.37 in paragonite, 2.19 in chlorite, 2.24 in amphibole, 1.15 in garnet, 0.72 in titanite, and 1.30 in rutile. The distribution of Cr in the samples is very irregular, even at the scale of a single crystal. In all silicates, Cr enters octahedral sites replacing ^{VI}Al. In epidote, Cr is mainly located at the M1 site, and in most samples epidote preferentially incorporates Cr over Al in comparison to other silicates. Rare, small inclusions of chromian spinel with anomalously high Zn contents (up to 15.14 wt.% ZnO) are found in some of the silicate phases. We consider chromian spinel to be the source of Cr in these metasediments, which were deposited as beach placers. The conservation of the original, sedimentary heterogeneity in Cr distribution as well as the zoning pattern of Cr in epidote suggest very limited mobility of this element during metamorphism. The high concentration of Zn in relict inclusions of chromian spinel is interpreted as a passive enrichment.

Keywords: chromian minerals, detrital chromite, beach environment of deposition, metacarbonates, limited mobility of Cr, Betic Cordilleras, Spain.

SOMMAIRE

Certains lits de roches métacarbonatées du complexe de Nevado-Filábride, dans les Cordillères Bétiques du sud de l'Espagne, contiennent des quantités anormales de minéraux riches en Cr. Ceux-ci sont concentrés dans des couches très minces faisant partie de lits quelques mètres d'épaisseur, interlités avec d'autres types de roches (métapélites et métacarbonates) sans chrome. Les teneurs en Cr atteignent 5.74% (poids) de Cr₂O₃ dans l'épidote, 5.09% dans la muscovite phengitique, 1.37% dans la paragonite, 2.19% dans la chlorite, 2.24% dans l'amphibole, 1.15% dans le grenat, 0.72% dans la titanite, et 1.30% dans le rutile. La distribution du Cr dans les échantillons est très irrégulière, même à l'échelle d'un cristal unique. Dans tous les silicates, le Cr occupe les sites à coordination octaédrique, remplaçant ^{VI}Al. Dans l'épidote, le Cr occupe surtout le site M1, et dans la plupart des échantillons, c'est l'épidote qui est l'hôte préféré du Cr. De rares inclusions de spinelle chromifère, de taille minuscule et ayant des teneurs élevées de Zn (jusqu'à 15.14% ZnO), se trouvent dans certains des minéraux silicatés. A notre avis, le spinelle chromifère serait la source du Cr dans ces unités métasédimentaires, autrefois des alluvions littorales. La conservation de l'hétérogénéité originelle dans la distribution du Cr du précurseur sédimentaire, de même que la zonation de l'épidote en Cr, font penser que le Cr est très peu mobile pendant le métamorphisme. La teneur élevée du Zn dans les micro-inclusions de spinelle chromifère résulterait d'un enrichissement passif.

(Traduit par la Rédaction)

Mots-clés: minéraux chromifères, chromite détritique, environnement de déposition littoral, métacarbonates, mobilité limitée du Cr, Cordillères Bétiques, Espagne.

INTRODUCTION

GEOLOGICAL SETTING

Chromian minerals have been known to occur in metacarbonate rocks from the Nevado-Filábride Complex, in the Betic Cordilleras of Spain. Martín Ramos & Rodríguez Gallego (1982) and Puga *et al.* (1992) described chromian mica in marble, and interpreted it as the result of metasomatism induced by the occurrence of ultramafic rocks in contact with marble.

In general, the incorporation of Cr in metamorphic silicate phases can be attributed to two processes: either Cr was transported from serpentinites and other ultramafic rocks by hydrothermal fluids (Cortesogno *et al.* 1981, Martín Ramos *et al.* 1979, Max *et al.* 1983, Pan & Fleet 1989, Grundmann & Morteani 1989), or new metamorphic minerals replaced previous minerals (usually chromite) and incorporated Cr in their structure (Ward 1984, Kerrich *et al.* 1987, Bertolani *et al.* 1991, Gil Iburguchi *et al.* 1991, Pan & Fleet 1991).

The concentration of Cr in sediments is possible by adsorption on or incorporation in crystals of clay minerals derived from weathering of mafic and ultramafic rocks (Garver & Royce 1993, Treloar 1987a) or from organic matter (Ottaway *et al.* 1994); these minerals were then transformed into other silicate minerals during metamorphism. Alternatively, Cr can be concentrated as detrital chromite, as previously described by Winkler & Bernoulli (1986), Bernoulli & Winkler (1990), Garver & Royce (1993), and Utter (1978). Such a concentration can be preserved in metasediments as layers of very chromium-rich minerals.

In the rocks studied, crystals of chromium-rich silicates are concentrated in well-defined layers within the metasedimentary sequence, and they commonly contain small inclusions of chromian spinel. In addition, the distribution of chromium is controlled by the location of the spinel inclusions. These textural and chemical features indicate that the most likely source of the Cr is chromite present as detrital grains, most likely from beaches, where this type of concentration in thin layers or beds is a common feature, produced by hydraulic sorting (Wilson 1975). This interpretation is consistent with a shallow marine environment, as proposed for the uppermost Nevado-Filábride metasedimentary sequence by Gómez-Pugnaire (1981), Gómez-Pugnaire & Cámara (1990), and de Jong & Bakker (1991).

We have attempted to resolve certain questions regarding the crystal-chemical behavior of Cr in some silicate minerals and the limited mobility of this element during metamorphism. We also present evidence for a passive enrichment of Zn in chromian spinel, *i.e.*, by decreasing the modal amount of spinel by mineral reactions, where Zn is not incorporated into the reaction products.

The Betic Cordilleras (Fig. 1a) are made up of several tectonic domains, among which are the Internal Zones (Fig. 1b), which consist of three complexes (in ascending order): the Nevado-Filábride, the Alpujárride, and the Maláguide (Egeler & Simon 1969). The Cr-bearing minerals appear within the metacarbonate rocks, which form the upper part of the Mulhacén nappe of the Nevado-Filábride Complex (Fig. 1c). This nappe is a complicated lithological sequence consisting of several minor tectonic units. The lowest zone is made of graphitic micaschist with dark intercalations of marble and quartzite, and local intrusions of granite of variable thickness. The age of this zone is not precisely established, as fossils and radiometric dates are very scarce. A Paleozoic (Lafuste & Pavillon 1976, Priem *et al.* 1966) or Precambrian age (Gómez-Pugnaire *et al.* 1982) has been attributed to the lowest graphitic lithologies. The upper part of the Mulhacén nappe is comprised of a very thick pelitic-psammitic formation (Tahal Schists, Nijhuis 1964), with metacarbonate layers, meta-evaporites, and metabasites toward the top. The highest part contains marble, calc-schist, amphibolite, micaschist, and serpentinized ultramafic rocks. The contact between the Paleozoic (or older) metasediments and the Tahal Schists is of sedimentary origin (Gómez-Pugnaire *et al.* 1981) and, as a consequence, the Tahal Schists must be younger than the underlying rocks, but beyond this their age is unconstrained. The stratigraphic correlation with other, less strongly metamorphosed Betic complexes allows us to attribute a Permo-Triassic age to the Tahal Schists, and a Triassic or younger age for the Cr-bearing metacarbonates at the top of the Mulhacén nappe.

Although the depositional environment of the Tahal Schists and the overlying metasediments is especially relevant for the geodynamic interpretation of the Nevado-Filábride Complex, there is no clear evidence indicating the origin of the sequence. Gómez-Pugnaire (1981) and de Jong & Bakker (1991) proposed a continental or transitional continental - shallow-marine environment for the deposition of the Tahal Schists. The metapelites directly above the Tahal Schists contain pseudomorphs after gypsum and scapolite porphyroblasts with anhydrite, barite, sylvite, and halite inclusions that reflect an original chemical composition typical of evaporitic sediments (Gómez-Pugnaire & Cámara 1990, Gómez-Pugnaire *et al.* 1994). The marbles and calc-schists from the top of the sequence have been interpreted as reefs in the border of a lagoon, where anoxic and hypersaline conditions caused the deposition of bituminous muds, evaporites and dolostones (de Jong & Bakker 1991). The sedimentary conditions we have deduced in this paper from the Cr-bearing metacarbonates also indicate a shallow-marine environment for the marble from the

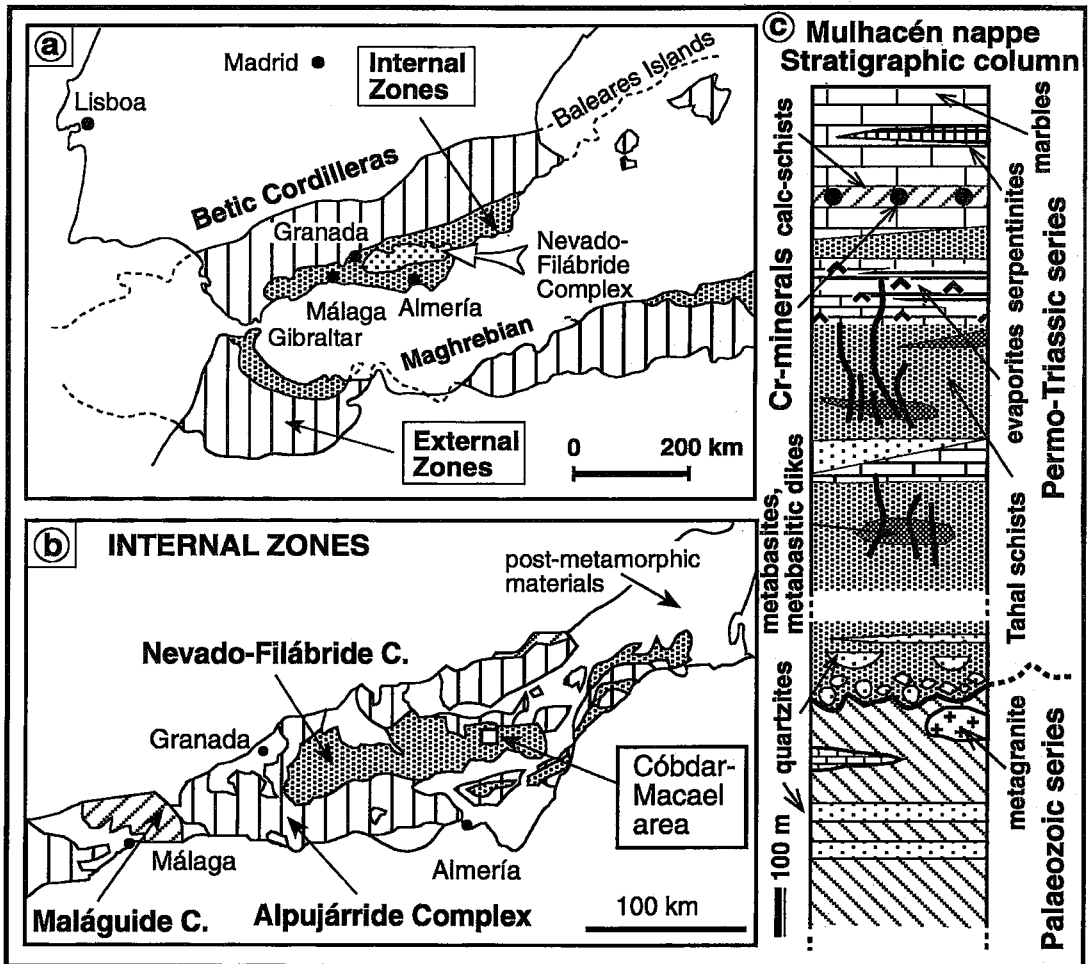


FIG. 1. a) Major tectonic units of the Western Mediterranean (southern Spain and northern Africa). b) Tectonic units of the Internal Zones of the Betic Cordilleras. c) Stratigraphic column of the Mulhacén nappe of the Nevado-Filábride Complex in the Córdar-Chercos area. The chromium-rich layers are indicated by dots.

highest part of the Mulhacén nappe sequence.

The metamorphic evolution of the Nevado-Filábride Complex rocks is not simple; it reveals the superposition of Alpine and pre-Alpine events (probably related to the Hercynian orogeny). The metamorphic and tectonic effects of both events have only been identified in the Paleozoic units. The assemblages of Cr minerals in the area studied appear in the Triassic series that have been affected only by Alpine metamorphism. This metamorphism developed in three stages; the first one took place under high pressure (~20 kbar) and at temperatures near 600°C, producing eclogites and blueschists in metabasites and kyanite + phengite + talc in metapelites (Cámara & Gómez-Pugnaire 1993). It was followed by a medium-pressure

(6.5 kbar) event at similar temperatures (Gómez-Pugnaire 1979). The final stage of metamorphism occurred under low pressure and temperature (Nijhuis 1964, Puga & Díaz de Federico 1978, Gómez-Pugnaire & Fernández Soler 1987).

OCCURRENCE OF Cr-BEARING MINERALS

The chromian minerals described appear in the marble and calc-schist sequence studied by Voet (1967), in the Córdar-Chercos area (Sierra de los Filabres, Betic Cordilleras, Fig. 2). This sequence overlies a thick unit of marble (Córdar marble, Voet 1967) separating it from the Tahal Schists. The marble and calc-schist sequence, commonly rich in amphibole

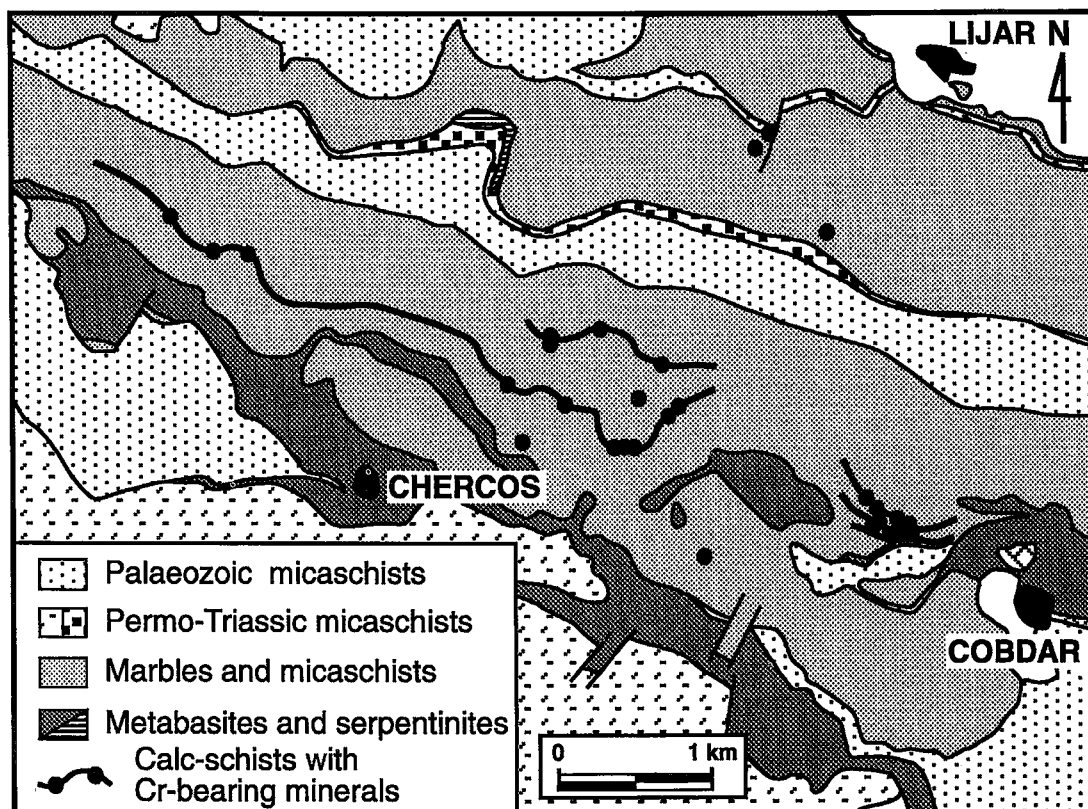


FIG. 2. Geological sketch-map of the C6bdar-Chercos area (modified from Voet 1967). Chromian minerals occur in small folded layers of calc-schists and marbles.

and garnet, consists of layers of pure marble of variable thickness, of pelitic rocks with and without graphite, and of garnet-rich quartzite.

Chromian minerals are present in only some of the metacarbonate layers from this sequence, most commonly in calc-schists. They are particularly abundant in the rocks near or directly in contact with quartz- and garnet-rich dark micaschists. These minerals are commonly concentrated in very thin layers, some only a few millimeters thick, where emerald-green muscovite ("fuchsite") is especially conspicuous (Fig. 3). These thin layers occur in beds a few meters thick, which can be followed laterally for several kilometers and which are interbedded with metapelite and metacarbonate devoid of Cr. In many places where the foliation is lost, the rocks acquire a more granoblastic appearance, and the Cr-rich minerals are coarsened.

Most of the marble is calcitic and has a uniform granoblastic texture. In metacarbonate rocks with Cr-minerals, texture and composition are more variable. Although a granoblastic texture is still predominant,

evidence of deformation, such as sutured grain-boundaries, preferred orientation of grains, mortar texture, and deformation twins, also is common. Calcite is the most common carbonate phase, but dolomite, with a variable Fe content, is commonly associated with the Cr-rich silicate minerals. Limonitization has widely affected calc-schists and intercalated layers of marble. Quartz is present in variable amounts in most of the samples studied, and is usually concentrated in layers or irregular aggregates. Table 1 shows the mineral assemblages developed during the successive metamorphic stages.

Epidote-group minerals are very common in calc-schist and impure marble. We have identified both Cr-poor and Cr-rich varieties. Chromian epidote crystals commonly attain up to 3 mm in length, but in a few outcrops intense green zoisite may attain up to 2 cm. The grains are tabular, almost acicular, or skeletal. With the exception of green, Fe-poor zoisite, chromian epidote is strongly pleochroic pale or greenish yellow to strong yellow. Crystals of chromium-poor epidote

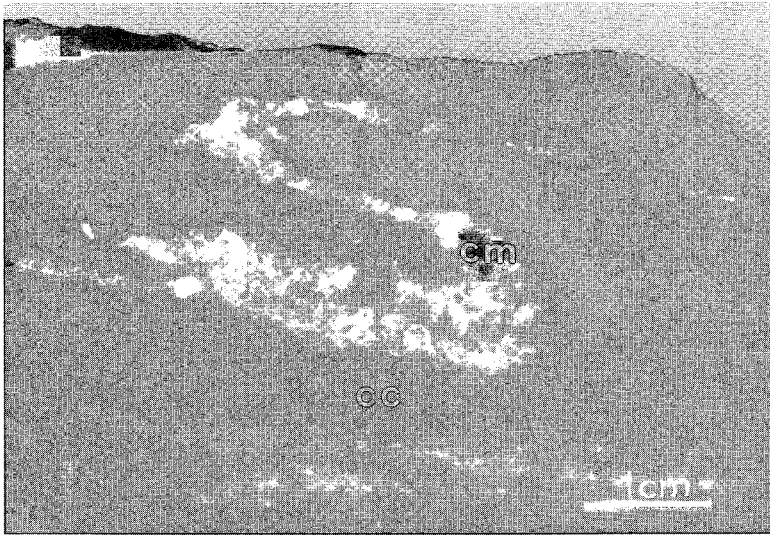


FIG. 3. Photograph of a hand specimen of white calcite marble (cc) with a small folded layer of chromian phengite and other Cr-rich minerals (cm).

are usually small, rounded or subhedral, and appear as aggregates or in veins cross-cutting the main metamorphic assemblages. Both Cr-rich and Cr-poor grains may occur together in the same thin section.

Epidote and actinolitic or hornblending amphibole coexist in most of the samples. They may have reacted to chlorite, calcite and quartz, or appear as inclusions within each other. Grains of chromian epidote also

may contain many inclusions of dolomite (generally idioblastic), titanite, pyrite, chalcopyrite, ilmenite, and small, irregular grains of chromian spinel (Figs. 4, 5). More rarely, very small, acicular inclusions of amphibole may appear. They show a strong preferred orientation or form relict folds within the grains of chromian epidote, thus indicating a relict phase of an older metamorphism, possibly the first Alpine high-pressure stage. Inclusions of chromian epidote within sodic plagioclase blasts are very rare. However, Cr-free epidote occurring as inclusions in plagioclase is widespread in many metacarbonate rocks from the Nevado-Filábride Complex.

Phengitic muscovite is the most common, and in many instances the only silicate mineral in these rocks. There are no textural differences between Cr-poor and Cr-rich ("fuchsite") coexisting muscovites, except in the strong greenish and bluish pleochroism. As in the case of epidote, small inclusions of chromian spinel may be found in some grains of Cr-rich phengite.

Paragonite is much scarcer than phengitic muscovite. It appears as fine-grained crystals that form aggregates, and are usually in contact with phengite. Chromian paragonite is rare and displays weak greenish pleochroism.

Chromian chlorite is an abundant phase in most of the samples studied. It commonly appears as large radiating aggregates with no preferred orientation. In some cases, it is texturally evident that it was produced by a reaction between amphibole and epidote. The presence of small inclusions of chromian spinel in a few grains suggests, however, that chlorite also grew

TABLE 1. MINERAL ASSEMBLAGES DEVELOPED AT EACH METAMORPHIC STAGE

MINERALS	FIRST METAMORPHIC STAGE	SECOND METAMORPHIC STAGE	THIRD METAMORPHIC STAGE
	(20 kbar, 600°C)	(8-7 kbar, 650°C)	(3.5 kbar, 300-350°C)
Amphibole	-----		----
Apatite		---	
Calcite			
Chlorite	-----		
Dolomite		---	
Epidote			-----
Garnet		---	
Ilmenite			-----
Magnetite			
Muscovite			-----
Paragonite	-----		
Quartz			
Pyrite			
Rutile		---	
Spinel			
Titanite			---

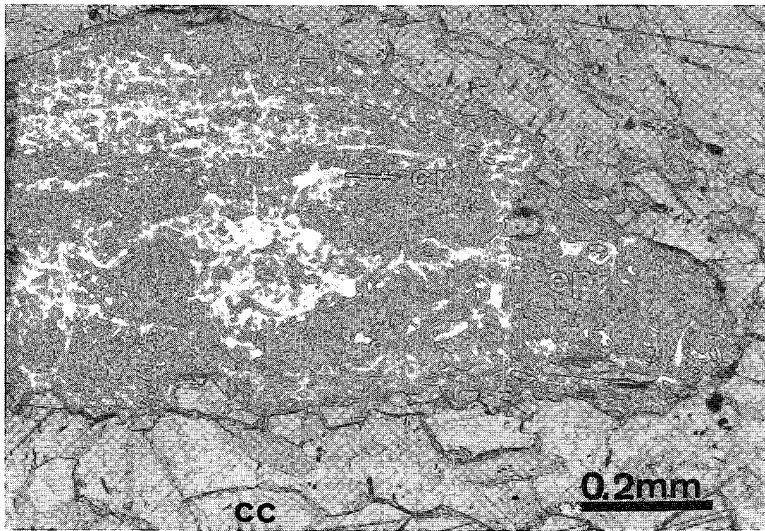


FIG. 4. Microphotograph of chromian epidote (ep) with inclusions (dark spots in the central part of the epidote grain: cr) of chromite, ilmenite and magnetite (cc: calcite; plane-polarized light; sample number 1013-3).

earlier, together with the other chromian silicates. In a few samples, intense later chloritization took place, corroding epidote and mica grains.

Amphibole, with high contents of Cr, is a very common phase coexisting with other chromian silicates. It is intensely green, which makes the rocks very dark. The amphibole crystals are concentrated in layers, with a good preferred orientation, or have

developed in radiating aggregates, with crystals up to 2 cm long. In thin section, amphibole displays strong green-to-blue pleochroism and is associated with other chromian silicates, especially epidote and chlorite.

Garnet is very scarce in rocks containing chromian minerals, but is common in most of the Cr-free calc-schists from the area. Chromian garnet is rounded and commonly corroded along its rim by chlorite. In some

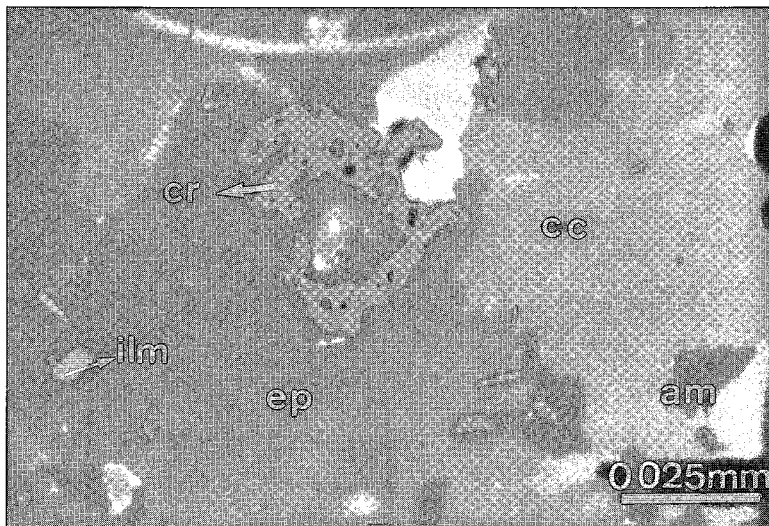


FIG. 5. Microphotograph of an inclusion of skeletal chromite (cr) in chromian epidote (ep). Other small white inclusions are ilmenite (ilm) (cc: calcite, am: amphibole, reflected light; sample number 1013-3).

grains, inclusions of yellow epidote and amphibole have been found, but no inclusions of chromian spinel could be detected.

Chromian spinel occurs as rare, small, round or skeletal, brown inclusions in chromian silicates, especially epidote (Figs. 4, 5). They occur together with elongate grains of ilmenite and round grains of magnetite. Chromian spinel has not yet been found as isolated grains within the carbonate matrix of the rocks.

Titanite and *rutile* (isolated or in aggregates) are present in small amounts in most of the samples. Titanite appears as grains with variable size and shape (subidioblastic to skeletal) in the carbonate matrix and also as common inclusions within epidote, amphibole, and phengitic muscovite. In some samples, titanite is partially replaced by rutile, calcite, and quartz.

MINERAL CHEMISTRY

Minerals were analyzed with an automated Camebax electron microprobe (wavelength-dispersion system) with natural minerals and synthetic materials as standards (Na: albite, K: orthoclase, Ca and Si:

TABLE 2. CHEMICAL COMPOSITION OF EPIDOTE-GROUP MINERALS, PHENGITE AND PARAGONITE

	1	2	3	4	5	6	7	8
Sample	1013-3	1013-6	1013-16	1013-16	1013-16	1013-16	FEPI0	1013-196
SiO ₂	37.97	38.35	39.15	37.36	49.09	49.43	49.16	46.94
TiO ₂	0.03	0.13	0.14	0.08	0.30	0.27	0.10	0.06
Cr ₂ O ₃	0.91	2.39	5.74	10.08	1.15	5.09	1.62	1.37
Al ₂ O ₃	21.53	27.86	25.76	24.57	29.88	26.15	26.85	38.51
Fe ₂ O ₃	14.44	4.31	3.15	3.85	-	-	-	-
FeO	-	-	-	-	1.16	1.13	4.33	0.00
MnO	0.16	0.30	0.12	0.06	0.03	0.00	0.00	0.02
MgO	0.00	0.08	0.03	0.13	3.07	2.99	2.52	0.43
CaO	23.19	23.74	23.95	23.23	0.05	0.14	0.00	0.43
Na ₂ O	0.02	0.00	0.09	0.02	1.03	0.50	0.59	5.34
K ₂ O	0.00	0.00	0.00	0.03	9.09	9.63	8.80	2.63
TOTAL	98.25	97.16	98.13	99.41	94.85	95.33	93.97	95.736
Si	3.034	3.003	3.053	2.926	6.536	6.643	6.700	6.016
IVAl	-	-	-	0.074	1.464	1.357	1.300	1.984
VIAl	2.028	2.571	2.367	2.120	3.224	2.784	3.013	3.834
Fe ³⁺	0.868	0.254	0.185	0.227	-	-	-	-
Fe ²⁺	-	-	-	-	0.129	0.127	0.494	0.000
Cr	0.057	0.148	0.354	0.624	0.121	0.541	0.175	0.140
Ti	0.002	0.008	0.008	0.005	0.030	0.027	0.010	0.006
Mn	0.011	0.020	0.008	0.001	0.003	0.000	0.000	0.002
Mg	0.000	0.009	0.003	0.007	0.609	0.599	0.512	0.082
Oct	2.966	3.010	2.926	2.984	4.117	4.078	4.203	4.064
Ca	1.985	1.991	2.001	1.949	0.007	0.020	0.000	0.060
Na	0.003	0.000	0.014	0.003	0.266	0.130	0.156	1.328
K	0.000	0.000	0.000	0.003	1.544	1.651	1.530	0.430

1, 2, 3 and 4: epidote minerals (cations calculated on the basis of 12.5 O)
 5, 6 and 7: phengite (cations calculated on the basis of 22 O)
 8: paragonite (cations calculated on the basis of 22 O); electron-microprobe data.

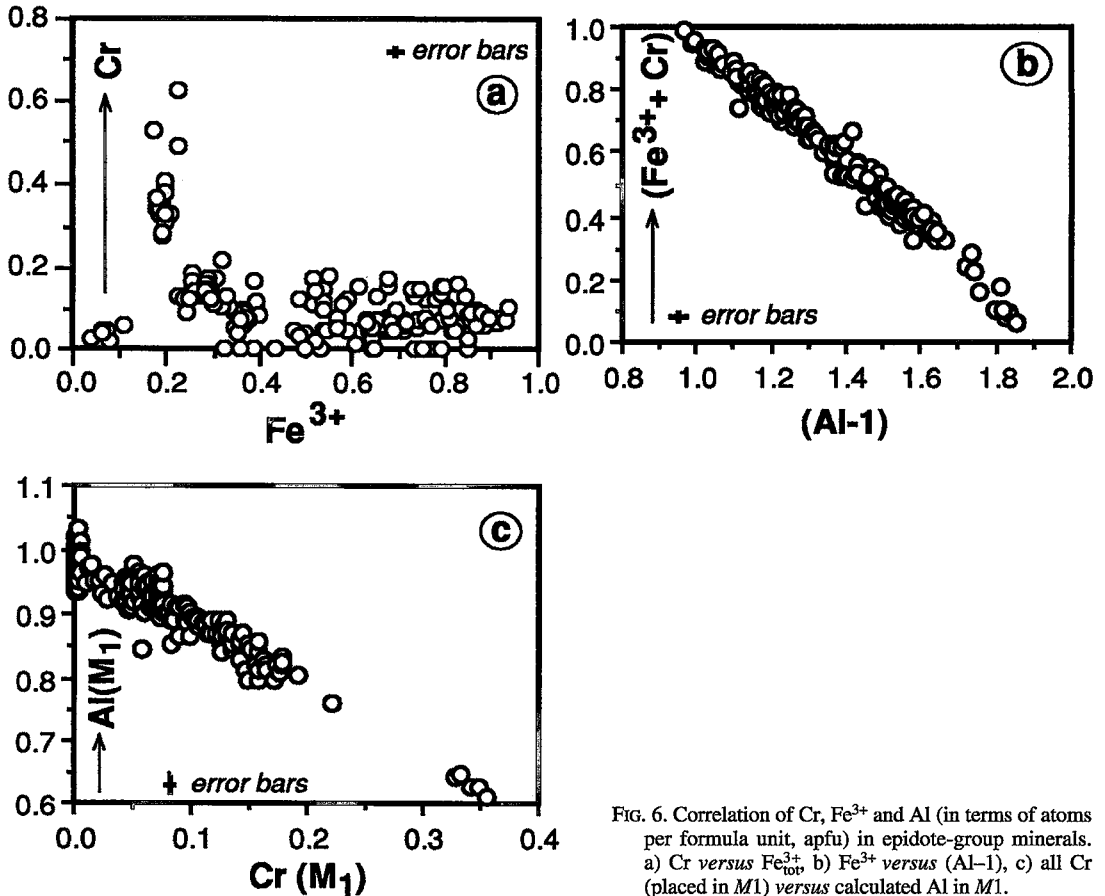


FIG. 6. Correlation of Cr, Fe³⁺ and Al (in terms of atoms per formula unit, apfu) in epidote-group minerals. a) Cr versus Fe_{tot}³⁺, b) Fe³⁺ versus (Al-1), c) all Cr (placed in M₁) versus calculated Al in M₁.

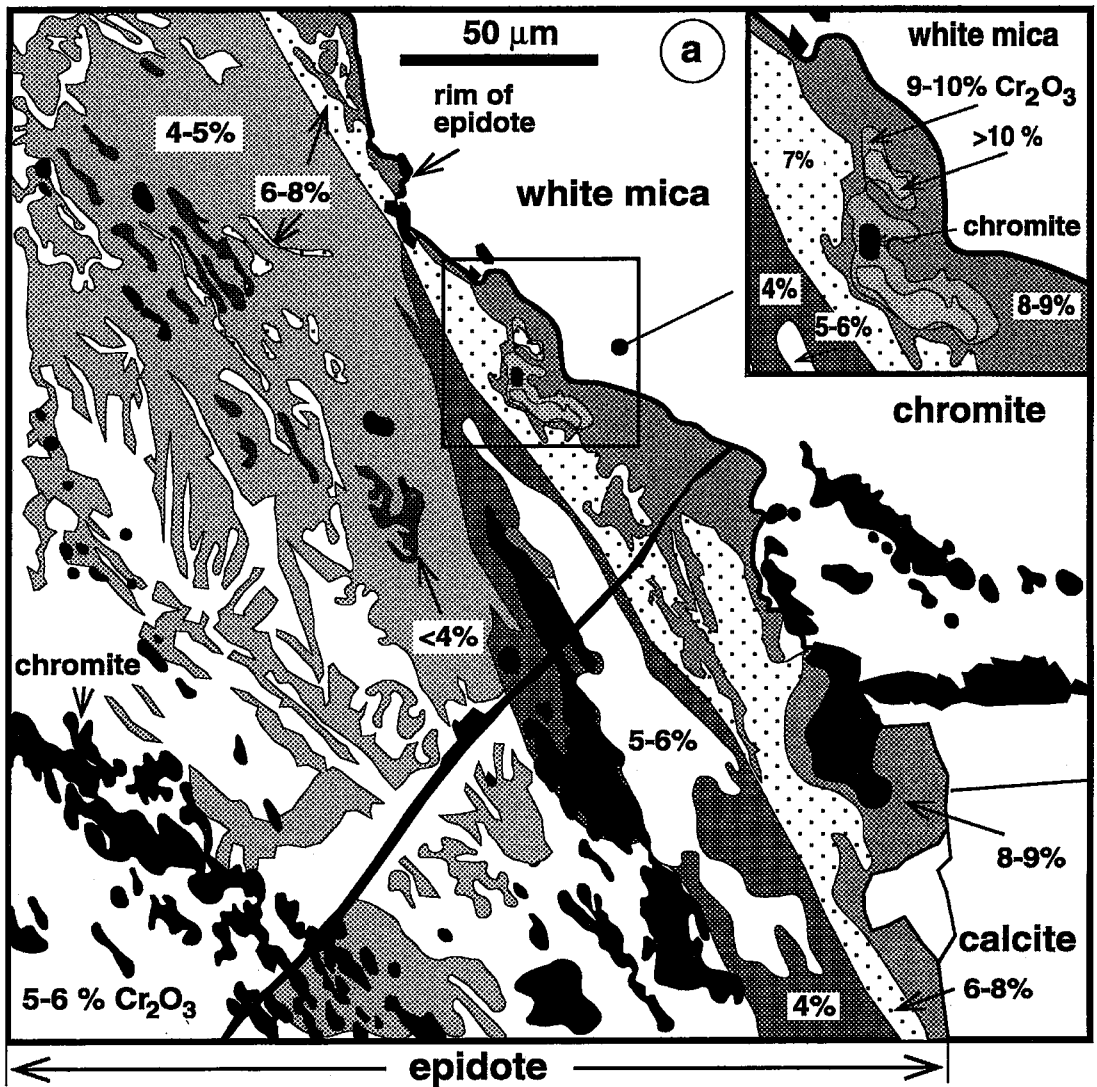


Figure 7a

wollastonite, Al: Al_2O_3 , Mg: MgO , Fe: FeO , Mn: Mn, Ti: TiO_2 , Cr: chromite, Zn: hercynite) at 15 kV, 20 nA, using the PAP correction at ZELMI (Technical University of Berlin). Counting times were 10 s for Na, Mg, Si, Al, and K, and 20 s for Fe, Cr, Zn, Mn and Ca. Additional data were obtained at the electron-microprobe laboratories of Granada, Padua and Zürich under similar conditions. Analytical precision is 1.25% for elements present at levels greater than 10 wt.%, 2% for elements between 1 and 10 wt.%, and 2.5% for elements amounting to less than 1.0 wt.%.

Epidote-group minerals

The dominant epidote-group mineral is monoclinic, as suggested by its oblique extinction. This is consistent with its high Fe_2O_3 content (Table 2) (Franz & Selverstone 1992). Aggregates of orthorhombic zoisite have values lower than ~ 1.0 wt.% Fe_2O_3 . The chemical composition of clinozoisite is characterized by high Cr contents (up to 5.74 wt.% Cr_2O_3). More typical concentrations of Cr_2O_3 are about 2 wt.%. Values for Ti, Mn, Mg, Na, and K are very low. Significant

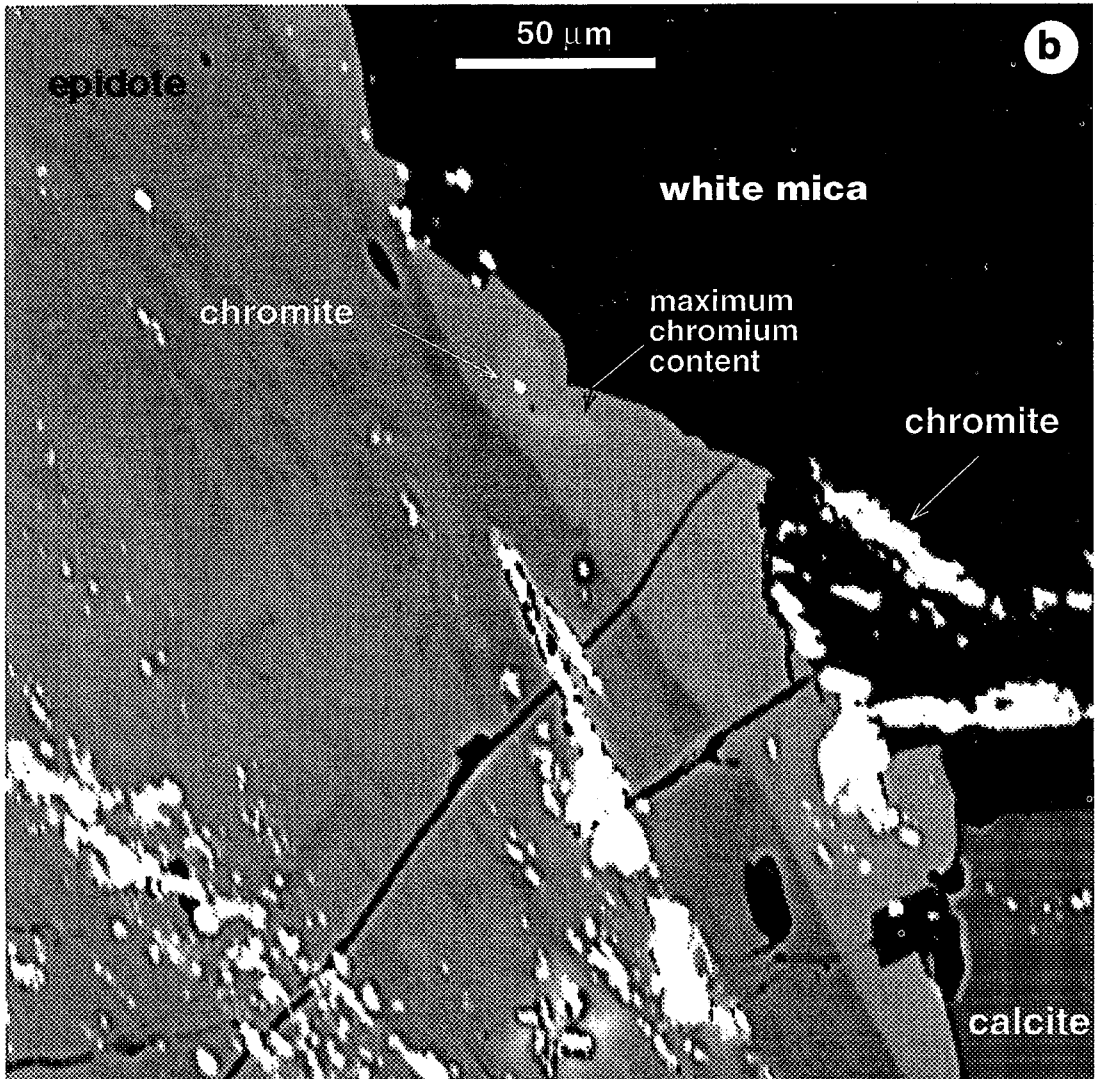


FIG. 7. Pattern of zoning in epidote (sample number 1013-3). a) Drawing from back-scattered electron (BSE) image showing a part of a large crystal of epidote in white mica and calcite. Note that the variation in grey shading in BSE images in epidote is due to a combined effect of Cr- and Fe-content, but in this example it is strongly dominated by Cr. The chromium content in epidote is given in wt.% Cr_2O_3 , and was measured in spot analyses. In the inset, the pattern of the rim area is shown in more detail. b) Labeled photograph covering the area in a).

values for rare-earth elements (La and Ce) were detected in the core of some Cr-free grains, indicating solid solutions with allanite.

The structural formulas, like those obtained by other authors (Grapes 1981, Treloar 1987b, Pan & Fleet 1989), also show small deviations from the theoretical values for Si and total octahedrally coordinated cations. The meaning of these anomalies and their possible relationship with Cr content is not clear. For Si values, anomalies could be related to the small $\text{SiK}\alpha + \text{CaK}\alpha$ combined peak that overlaps the $\text{CrK}\alpha$

peak, as described by Treloar (1987a).

Location of Cr in octahedral sites in epidote

Epidote and the hypothetical end-member $\text{Ca}_2\text{CrAl}_2\text{Si}_3\text{O}_{12}(\text{OH})$ (tawmawite) form a solid-solution series. There are uncertainties about the exact distribution of the cations Al, Fe^{3+} and Cr among the three different octahedral sites $M1$, $M2$, and $M3$, which occur in equal proportions in the epidote structure. There is general agreement about the complete

occupancy of the *M2* site by Al, but whether Fe³⁺ substitutes for Al in *M1* or in *M3*, and the position of Cr³⁺, are not well known. Grapes (1981) proposed that both Cr and Fe³⁺ substitutions take place in the *M3* site, as they are crystallochemically similar. On the other hand, Treloar (1987b), as well as Burns & Strens (1967), suggested that Cr has a strong preference for the *M1* site, whereas Fe³⁺ occupies the *M3* site. Mössbauer spectroscopy data confirm that for compositions with less than 0.8 Fe³⁺ per formula unit, no Fe³⁺ is detected in the *M1* site (Dollase 1973, Gabe *et al.* 1973).

We have drawn different correlation diagrams to clarify the relation between Cr³⁺ and the other octahedrally coordinated cations Al and Fe³⁺. Figure 6a shows no correlation of Cr with Fe³⁺, but there is a very good negative correlation between (Al-1) and (Fe³⁺ + Cr) (Fig. 6b). We used "(Al-1)" because we assume that the *M2* position is completely filled with Al. The inverse correlation confirms, in agreement with other authors (Dollase 1971, Burns & Burns 1975), that Fe³⁺ and Cr substitute for Al in octahedrally coordinated sites (the presence of ^{IV}Al can be disregarded: Deer *et al.* 1986).

Cation distributions in octahedrally coordinated sites for our epidote compositions, assuming that the hypothesis of Burns & Strens (1967) and Treloar (1987b) is correct, indicate that Cr is in the *M1* (Cr_{*M1*}) site, and Fe³⁺ plus the rest of the minor octahedrally coordinated cations occupy the *M3* site (Tot_{*M3*}). The Al content for both *M1* and *M3* sites (Al_{*M1*} and Al_{*M3*}, respectively) were calculated by assuming that the *M2* site is completely filled with Al, and by distributing the remaining Al between the *M1* and *M3* sites:

$$\begin{aligned} Al_{M1} &= (1 - Cr_{M1})(Al-1)/(1 - Cr_{M1}) + (1 - Tot_{M3}) \\ Al_{M3} &= (1 - Tot_{M3})(Al-1)/(1 - Cr_{M1}) + (1 - Tot_{M3}); \end{aligned}$$

where the octahedrally coordinated positions are not completely filled, the Al distribution was made proportionally to the actual total content of octahedrally coordinated cations in each case. The results show an excellent correlation between Cr_{*M1*} and Al_{*M1*} (Fig. 6c), and also between Tot_{*M3*} and Al_{*M3*} (not shown). These correlations confirm that the calculated number of cations per formula unit can be distributed ideally according to the hypothesis of Burns & Strens (1967).

Zoning in Cr content in epidote

A comparison of compositions of epidote from seven different samples shows a very irregular distribution of Cr on a small scale. Chromium-rich and Cr-poor or Cr-free epidote grains may coexist in the same thin section. The greatest and smallest differences in Cr content in one thin section are 5.61 wt.% Cr₂O₃ and 0.51 wt.% Cr₂O₃, respectively. For individual grains, the differences in contents reach 2.96 wt.%

Cr₂O₃, and important differences invariably occur in grains with relict inclusions of chromian spinel. Zinc-rich spinel commonly leads to a higher Cr content in the surrounding epidote than a Zn-poor type. Large grains of epidote are invariably much more compositionally heterogeneous than the smaller ones. Figure 7 shows an example of this zoning. In this case, the rim is enriched in Cr (> 7 wt.% Cr₂O₃) compared to the central part of the crystal (4–6 wt.% Cr₂O₃), though there are also many areas with higher Cr-concentrations in the central part. They occur in the vicinity of chromite inclusions, and we observe an increase in Cr content of the epidote toward chromite (see inset in Fig. 7, an enlarged part of the rim area). However, there are also intergrowths of chromite with epidote of low Cr-content (see central part of the crystal near large grain of chromite).

Phengite

Phengite has a variable Cr content (Table 2), with a high value of 5.09 wt.% Cr₂O₃. The distribution of Cr is irregular on a thin section scale, but individual grains are usually more homogeneous than epidote, even if they contain chromite inclusions. The composition can be described by the coupled substitution: Si + (Mg + Fe) = ^{IV}Al + (^{VI}Al + Cr + Ti) (Pan & Fleet 1991).

Figure 8a shows important overall variation in both X_{Mg} [= Mg/(Mg + Fe²⁺_{tot}), all Fe calculated as Fe²⁺] and Si. Although no textural differences are evident among grains of different composition, the important variation in Si within each sample and its strong positive correlation with X_{Mg} suggest that the phengite grew in several metamorphic episodes along the decompression path of the rocks (Massonne & Schreyer 1987). Preservation of these trends may be due to a low rate of re-equilibration for muscovite. The wide variation of X_{Mg} among individual samples also reflects the influence of local bulk composition (López Sánchez-Vizcaíno 1994). The Cr occupies an octahedrally coordinated position, as the negative correlation between Cr and ^{VI}Al suggests (Fig. 8b). The negative correlation observed between Si and X_{Na} [= Na/(Na + K + Ca)] (not shown) is the result of the increase in Na content in mica with decreasing pressure and with the final growth of paragonite. This behavior is similar to that in phengite found in the alternating metapelites and metabasites that show several other lines of textural and chemical evidence for polyphase metamorphism (López Sánchez-Vizcaíno 1994).

Paragonite

The Cr content of paragonite (up to 1.37 wt.% Cr₂O₃) is lower than that of phengite. Given the good negative correlation between ^{VI}Al and Cr (Fig. 8b), it

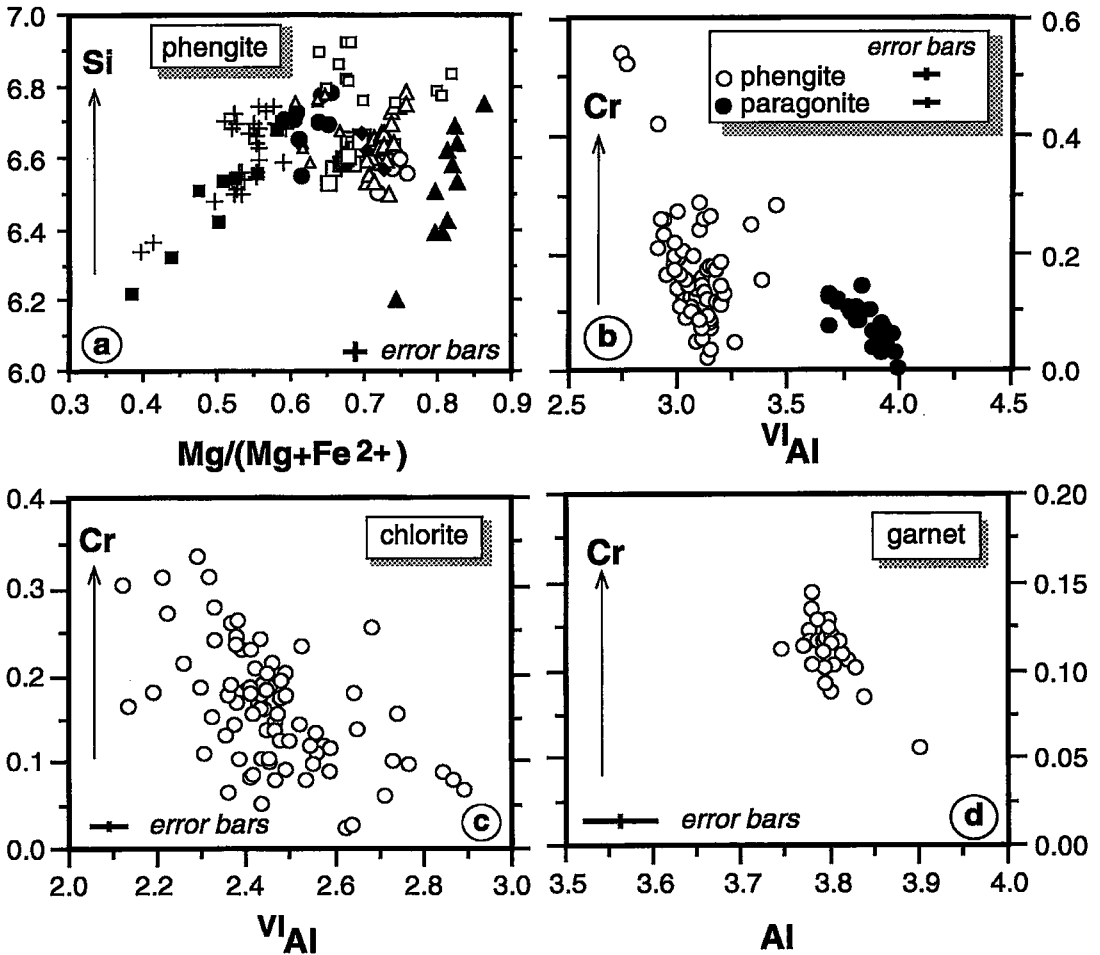


FIG. 8. a) $Mg/(Mg + Fe^{2+}_{tot})$ ratio of phengite in individual samples, correlated with Si in apfu (symbols: black triangles: 1013-16, white triangles: 1013-123, black circles: 1013-39, white circles: 1013-15, black squares: 1013-21, large white squares: 1013-166, small white squares: 1013-163, crosses: FEP-10/1); the strong variation in $Mg/(Mg + Fe^{2+}_{tot})$ with Si, especially in samples 1013-21 and FEP-10/1, indicates crystallization over a range of P-T conditions. b) Cr versus VIAl in phengite and paragonite; phengite can contain considerably more chromium than paragonite. c) Cr versus VIAl in chlorite. d) Cr versus Al in garnet. Error bars were calculated assuming the analytical precision given in the text.

is clear that Cr must occupy an octahedrally coordinated position. The high K contents of paragonite (Table 2) and the continuity between paragonite and phengite in the $Na/(Na + K + Ca)$ versus Si diagram (not shown) may indicate an intergrowth with muscovitic mica below the resolution of the beam size of the electron microprobe. Alternatively, these minerals may have crystallized under conditions near the crest of the solvus between paragonite and phengite.

Chlorite

Both green clinocllore and green chamosite (Bailey 1988) are present. Clinocllore is much more abundant, and the two only coexist in one of twelve samples analyzed. There is a wide variation of X_{Mg} and Cr (up to 2.19 wt.% Cr_2O_3), related to the local bulk composition of the rock and to the composition of the reactant minerals that produced chlorite (*cf.* Laird

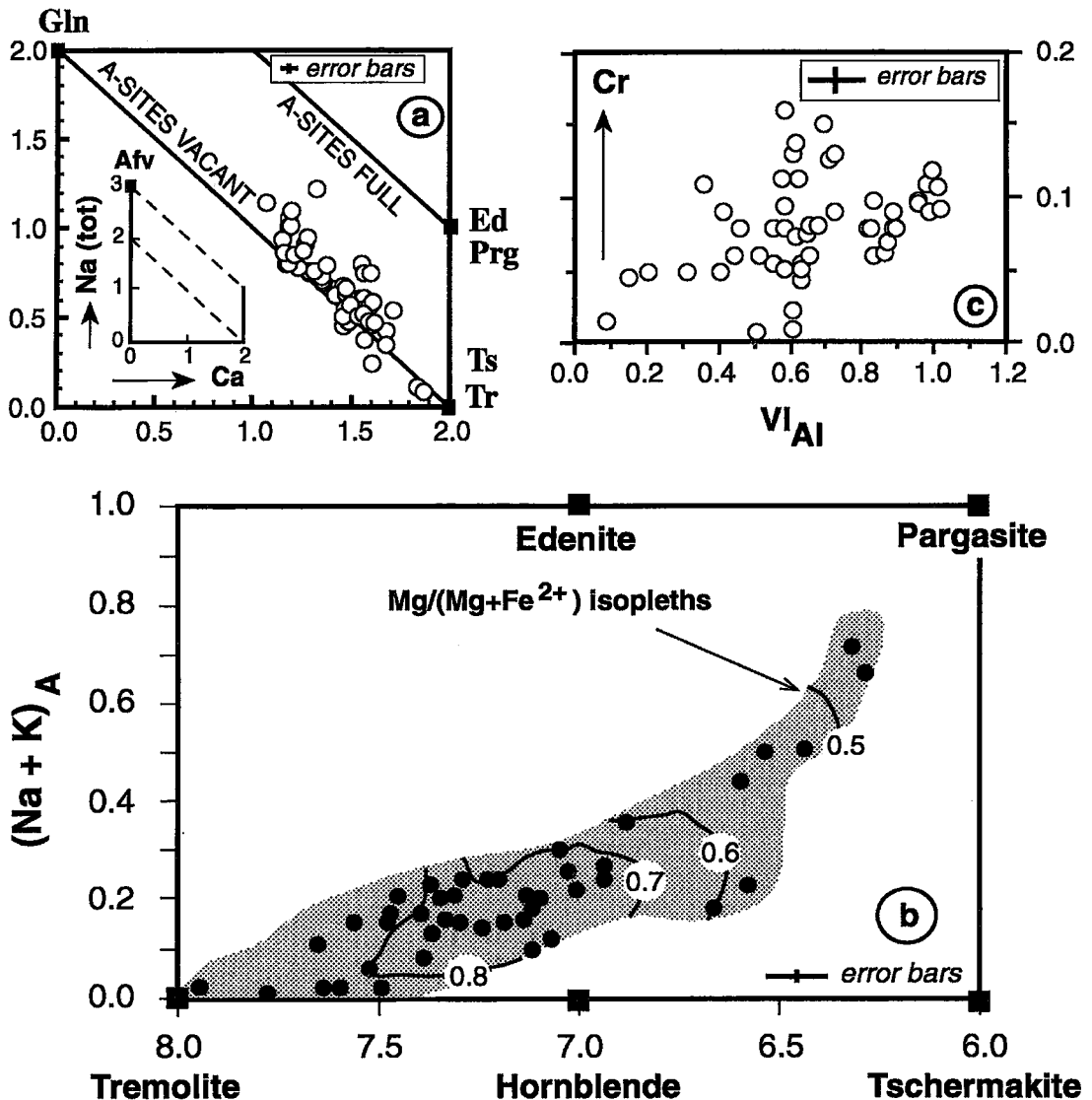


FIG. 9. Compositional variation of amphiboles in apfu. a) Amphiboles are calcic to sodic-calcic with pronounced glaucophane (Gln) and edenite (Ed) – pargasite (Prg) substitution. b) Variation in Tschermaks (Ts), pargasite (Prg), and edenite contents: isopleth of X_{Mg} increase systematically toward tremolite (Tr). c) Cr versus VI_{Al} .

1988). Cr occupies an octahedrally coordinated position according to the coupled substitution: $Si + (Mg + Fe) = ^{IV}Al + (^{VI}Al + Cr + Ti)$ (Table 3, Fig. 8c).

Amphibole

Table 3 and Figure 9 indicate a wide compositional range among tremolite, pargasite, glaucophane, and

tschermakite end-members, as well as in terms of Fe^{2+} -Mg. Fe^{2+} and Fe^{3+} were calculated using the method of Papike *et al.* (1974); we selected the average values between the maximum and minimum. Figure 9b [Si versus $(Na + K)_A$] shows the tschermakite ($Al_2Mg_{-1}Si_{-1}$) and edenite ($NaAlSi_{-1}$) substitution in the calcic amphiboles, as well as the distribution of $Mg/(Mg + Fe^{2+})$ isopleths. Note the posi-

TABLE 3. CHEMICAL COMPOSITION OF AMPHIBOLE AND CHLORITE

	1	2	3	4	5	6	7	8
Sample	1013-84	1013-3	1013-6	FEP10	FEP10	1013-16	1013-123	FEP10
SiO ₂	42.98	50.75	55.97	41.81	44.95	27.97	28.35	24.91
TiO ₂	0.33	0.08	0.00	0.16	0.08	0.01	0.04	0.08
Cr ₂ O ₃	2.24	0.41	0.14	0.91	0.79	2.19	0.19	0.40
Al ₂ O ₃	12.72	6.03	1.87	15.34	13.76	20.88	21.33	21.48
Fe ₂ O ₃	7.41	4.90	1.89	6.05	6.22	-	-	-
FeO	11.87	9.43	4.21	13.24	11.26	12.57	11.89	25.97
MnO	0.51	0.19	0.25	0.03	0.15	0.07	0.05	0.04
MgO	7.82	13.11	20.16	6.71	8.16	24.58	24.16	14.01
CaO	8.62	9.63	12.78	8.25	7.73	0.07	0.01	0.01
Na ₂ O	3.49	2.10	0.39	3.83	3.65	0.02	0.01	0.00
K ₂ O	0.54	0.22	0.02	0.56	0.45	0.00	0.01	0.05
TOTAL	98.53	96.85	97.69	96.89	97.20	88.36	86.04	86.95
Si	6.38	7.370	7.782	6.286	6.622	5.485	5.641	5.321
IVAl	1.62	0.630	0.218	1.714	1.378	2.515	2.359	2.679
VIAl	0.605	0.400	0.088	1.004	1.011	2.311	2.643	2.730
Fe ³⁺	0.828	0.540	0.198	0.684	0.690	-	-	-
Fe ²⁺	1.473	1.150	0.490	1.665	1.387	2.062	1.978	4.640
Cr	0.263	0.050	0.015	0.108	0.092	0.340	0.030	0.068
Ti	0.037	0.010	0.000	0.018	0.009	0.001	0.006	0.013
Mn	0.064	0.020	0.029	0.004	0.019	0.012	0.008	0.007
Mg	1.372	2.840	4.179	1.504	1.792	7.186	7.166	4.462
Ca	1.372	1.500	1.904	1.329	1.220	0.015	0.002	0.002
Na	0.628	0.500	0.096	0.671	0.780	0.008	0.004	0.000
Na	0.376	0.090	0.009	0.445	0.263	-	-	-
K	0.103	0.040	0.004	0.107	0.085	0.000	0.003	0.014

1, 2, 3, 4 and 5: amphibole (13 cations - (Na, Ca, K) and charge balance)
6, 7, 8: chlorite (cations calculated on the basis of 28 O); electron-microprobe data.

TABLE 4. CHEMICAL COMPOSITION OF GARNET, TITANITE, SPINEL AND RUTILE

	1	2	3		4	5	6	7
Sample	1013-84	1013-84	1013-15	Sample	1013-6	1013-6	1013-166	1013-166
SiO ₂	37.19	37.08	30.86	SiO ₂	1.17	1.14	0.05	0.02
TiO ₂	0.13	0.01	36.98	TiO ₂	0.08	1.14	97.57	99.00
Cr ₂ O ₃	1.15	0.46	0.72	Cr ₂ O ₃	49.03	39.54	1.30	0.13
Al ₂ O ₃	20.20	20.76	1.33	Al ₂ O ₃	8.14	20.89	0.00	0.00
Fe ₂ O ₃	-	-	0.76	Fe ₂ O ₃	4.37	0.60	0.34	0.86
FeO	29.84	28.52	-	FeO	29.2	17.96	-	-
MnO	3.24	4.61	0.04	MnO	0.50	0.49	0.00	0.00
MgO	1.26	1.44	0.00	MgO	0.89	0.99	0.03	0.00
CaO	8.63	8.30	29.07	CaO	0.87	1.46	0.62	0.02
Na ₂ O	0.00	0.00	0.02	Na ₂ O	0.00	0.00	-	-
K ₂ O	0.01	0.00	0.01	ZnO	1.60	15.14	-	-
TOTAL	101.66	101.19	99.79	TOTAL	95.86	98.75	99.91	100.03
Si	5.932	5.925	1.000	Si	0.040	0.040	0.000	0.000
IVAl	0.068	0.075	-	Al	0.350	0.840	0.000	0.000
VIAl	3.728	3.833	0.051	Fe ³⁺	0.120	0.000	0.003	0.009
Fe ³⁺	-	-	0.019	Fe ²⁺	0.900	0.510	-	-
Fe ²⁺	3.980	3.810	-	Cr	1.430	1.070	0.014	0.001
Cr	0.145	0.058	0.018	Ti	0.000	0.090	0.982	0.992
Ti	0.016	0.002	0.901	Mn	0.020	0.010	0.000	0.000
Mn	0.438	0.624	0.001	Mg	0.050	0.050	0.000	0.000
Mg	0.299	0.344	0.000	Ca	0.030	0.050	0.009	0.000
Ca	1.475	1.420	1.009	Ni	0.000	0.000	-	-
Na	0.000	0.001	0.001	Zn	0.040	0.380	-	-
K	0.002	0.000	0.000					

1 and 2: garnet (cations calculated on the basis of 24 O)

3: titanite (cations calculated after Franz & Spear 1985)

4 and 5: spinel (3 cations and charge balance)

6 and 7: rutile (cations calculated on the basis of 2 O); electron-microprobe data.

tive correlation between Fe substitution for Mg and $(Na + K)_A$. These amphibole compositions are similar to those described by Castelli (1991) in high-pressure marbles, and are much more complex than those reported in other regionally metamorphosed carbonate rocks (Ferry 1976, Hoschek 1980, Franz & Spear 1983).

Chromium content (<2.24 wt.% Cr₂O₃, but usually <1 wt.%) is relatively low compared to ^{VI}Al and Fe³⁺ (Fig. 9c). There are no Cr - Fe³⁺, Cr - ^{VI}Al, or ^{VI}Al - Fe³⁺ correlations, but an excellent negative correlation can be observed between (Fe³⁺, Cr, ^{VI}Al) and (Mg, Fe²⁺), as well as a positive one between (Fe³⁺, Cr, ^{VI}Al) and the ^{IV}Al content. All data suggest that the presence of Cr in these amphiboles can be explained by the Tschermak substitution (Mg, Fe²⁺) + Si = (Fe³⁺, Cr, ^{VI}Al) + ^{IV}Al.

Garnet

Garnet is chemically homogeneous (Table 4), with up to 66.4 mol.% almandine, 10.7% pyrope, 10% spessartine, 18.2% grossular, and 2.3% uvarovite. The garnet contains between 0.46 and 1.15 wt.% Cr₂O₃, the highest values coming from grains in contact with chromian epidote. The distribution of Cr and Al in the garnet shows a negative correlation (Fig. 8d).

Chromian spinel

The composition of chromian spinel (Table 4)

varies between 39.54 and 49.03 wt.% Cr₂O₃, between 17.96 and 29.94 wt.% FeO, and between 8.14 and 20.89 wt.% Al₂O₃. Titanium (1.14 wt.% TiO₂), Mn (0.56 wt.% MnO), and Mg (0.99 wt.% MgO) contents are much lower. Zinc varies between 1.79 and 15.14 wt.% ZnO. The spinel compositions can be defined in terms of the components chromite, hercynite, magnetite, franklinite, gahnite, and ZnCr₂O₄, represented by a modified spinel prism in which Mg (very scarce in our samples) has been replaced by Zn (Fig. 10a). Values of the ratio 2Fe³⁺/(2Fe³⁺ + Al + Cr) vary between 0 and 0.27. Projected data-points on the base of the prism show a solid solution between chromite and hercynite, with minor quantities of gahnite (Fig. 10b). Several crystals with a high content of gahnite were found, but only two were large enough for reliable quantitative analysis. The Cr content of spinel inclusions and their host minerals is in some cases inversely related. Spinel rich in Zn and poor in Cr is included in epidote that is very rich in Cr.

Titanite and rutile

The composition of titanite (Table 4) is characterized by Al contents of up to 2.35 wt.% Al₂O₃, significant Cr contents between 0.27 and 0.72 wt.% Cr₂O₃, and minor quantities of Fe³⁺ (all Fe assumed as Fe³⁺) substituting for Ti, as shown by a good correlation of Ti versus (Cr + Al + Fe³⁺). Rutile shows a high variability in Cr content (between 0.13 and 1.30 wt.% Cr₂O₃) in grains found close together in the same thin section.

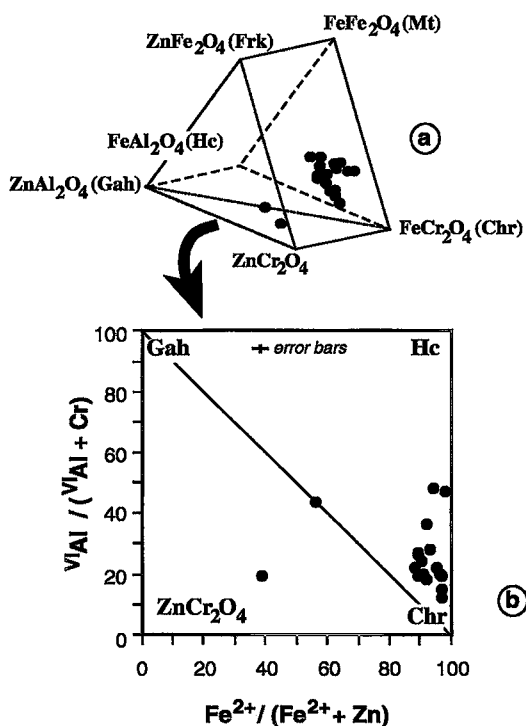


FIG. 10. Compositional variation of spinel inclusions in epidote. a) Spinel prism with the possible combination of (Zn, Fe²⁺) and (Al, Cr, Fe³⁺) end members, the concentration of Mg being low in these samples. b) Projection from ZnFe₂O₄ and FeFe₂O₄ (Chr: chromite, Mt: magnetite, Frk: franklinite, Hc: hercynite, Gah: gahnite).

DISCUSSION

Partitioning of Cr among coexisting phases

In order to obtain information on the behavior of Cr during metamorphism, we shall compare the Cr contents of different minerals. Epidote was selected as a reference mineral, because it is abundant in these rocks and it generally contains the highest amount of Cr. We do not compare the data of maximum Cr content in each phase, because this is controlled by the level of Cr saturation of the rock, as noted by Ward (1984) and Gil Ibarra *et al.* (1991). The saturation of Cr in respect to silicates is given if a chromian oxide is present as a phase. The presence of inclusions of chromian spinel and the increased Cr-content of associated silicates suggest that Cr-saturation might

have been reached only in contact with the inclusions. Instead, we compare data of coexisting silicates (Fig. 11). The data points in this figure pertain to minerals in contact, where the microprobe beam was placed 10 to 30 μm away from the grain boundary, and not in the vicinity of chromite inclusions. Care was taken to avoid grain boundaries with indications of a retrograde overprint.

The distribution of Cr can be defined as the Nernst partition coefficient [K_D = concentration of Cr in epidote (ppm) / concentration of Cr in other minerals (ppm)] (*e.g.*, Wood & Fraser 1977), assuming that this K_D is valid in a concentration range above the trace-element level (see McKay 1989, p. 54, for a discussion of this problem). This is the generally adopted procedure in geochemical investigations. In epidote–chlorite and epidote–amphibole pairs (Fig. 11a), Cr preferentially enters epidote, though not in all cases ($0.84 < K_D < 2.46$). In the epidote–muscovite pairs (Fig. 11b), K_D varies between 0.56 and 2, with a roughly equal number of points plotting above and below the $K_D = 1$ line. For the few epidote–garnet pairs, K_D is invariably between 1 and 2.

The distribution of Cr between epidote and coexisting chlorite, muscovite, amphibole and garnet can also be expressed on the basis of cation-exchange reactions and their corresponding equilibrium-constant (*e.g.*, Spear 1993). This allows one to describe the partitioning of Cr in relation to other cations. In order to distinguish it from the Nernst distribution coefficient, we call it K_{Ex} . These reactions involve the exchange of Al and Cr; K_{Ex} depends on the formulation of the inter-crystalline exchange-reactions and is generally defined as:

$$K_{Ex} = (X_{Al}^{Ep} \cdot X_{Cr}^{min}) / (X_{Cr}^{Ep} \cdot X_{Al}^{min}).$$

It also depends on the intracrystalline exchange on different sites, as will be discussed below. Two groups of minerals incorporate Cr: for amphibole and chlorite, the additive component (Thompson 1982) for the Cr–Al exchange is an Fe–Mg phase with small amounts of Al, whereas for garnet and muscovite, the additive component is an Al mineral with no Fe–Mg on the Al site (garnet) or small amounts only (phenigite).

For chlorite, there are two possibilities to formulate the exchange reaction, depending whether Cr substitution takes place in the sheet of octahedra of the interlayer (reaction 1a; exchange component is $interlayer_{Cr}^{interlayer}Al_{-1}$), or in the sheet of octahedra that is sandwiched between the sheets of tetrahedra (reaction 1b; exchange component is $VI_{Cr}^{interlayer}Mg_{VI}Mg_{-1}^{interlayer}Al_{-1}$). The two varieties of chlorite can be distinguished by their macroscopic color: Bailey (1988) described the color of the former as purple, that of the latter as green. The exchange reactions are:

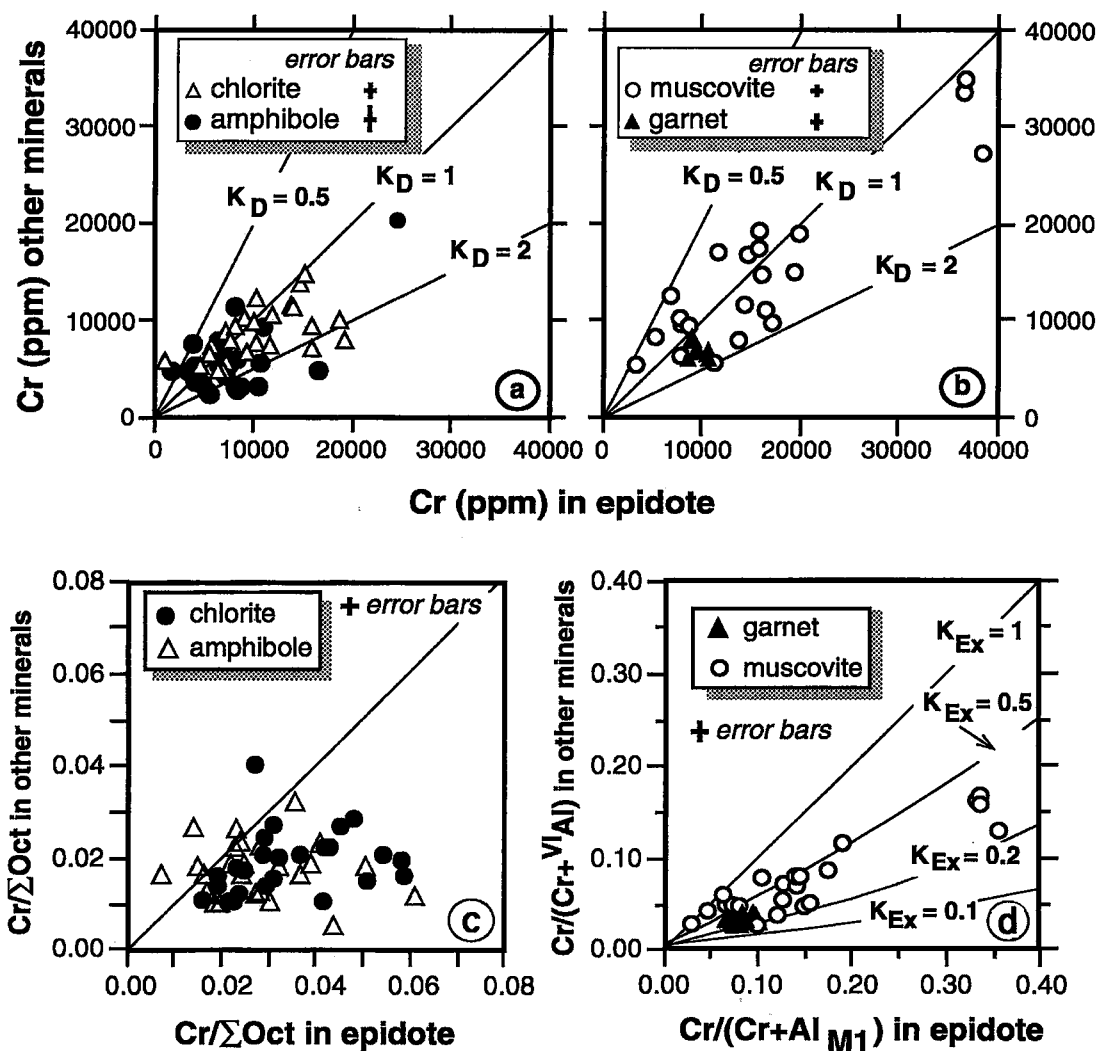
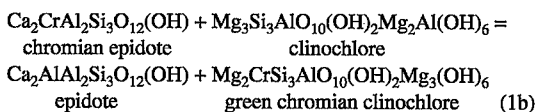
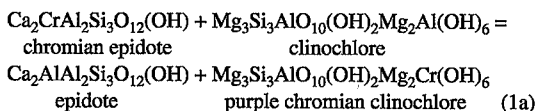


FIG. 11. Distribution of Cr between epidote and coexisting muscovite, garnet, amphibole, and chlorite. a) Cr in epidote *versus* Cr in chlorite and *versus* Cr in amphibole (in ppm). Lines represent the partition coefficients ($K_D = \text{Cr in epidote} / \text{Cr in other minerals}$). For both mineral pairs, most of the points concentrate in the epidote field or they plot very close to the line $K_D = 1$, but a greater dispersion can be observed in epidote–amphibole pairs. b) Cr in epidote *versus* Cr in muscovite and *versus* Cr in garnet (in ppm). In the first case, Cr does not enter preferentially in epidote, nor in muscovite. In the epidote–garnet pairs, all the points plot below the $K_D = 1$ line. c) and d) Cr distribution in terms of cation-exchange reactions; for definition of X_{Cr} , see text. Cr is preferentially incorporated in epidote, but this strongly depends on the formulation of X_{Cr} . Lines represent partition coefficients K_{Ex} (see text).



If the Tschermak substitution is restricted to one Al (or Cr) per formula unit, and if it is clear that the substitution takes place either according to reaction (1a) or (1b), X_{Cr} in chlorite could be defined as:

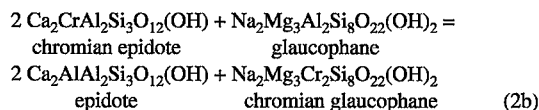
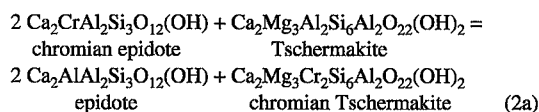
$$X_{Cr}^{\text{chl}} = \text{Cr} / (\text{Cr} + \text{interlayer Mg} - 2) \quad (1a)$$

or

$$X_{Cr}^{\text{chl}} = \text{Cr} / (\text{Cr} + \text{VI Mg} - 2) \quad (1b)$$

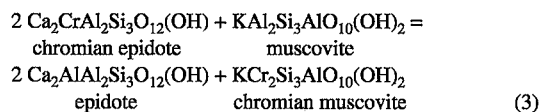
The chromian chlorite of the C6bdar area is green, and the dominant substitution would seem to be (1b). However, there can also always be a certain amount of substitution in the interlayer (1a). Since this intracrystalline distribution of cations and also the possible extent of Al-Tschermaks substitution are unknown, we must use as X_{Cr}^{chl} the ratio of Cr to the sum of all octahedrally coordinated cations, and the same for X_{Cr}^{ep} in Figure 11c. This figure shows an enrichment of Cr in epidote because of the large number of octahedrally coordinated positions in chlorite (and amphibole, see below) compared to epidote. If we use as X_{Cr} simply the ratio of Cr/(Cr + ^{VI}Al) (not shown), both amphibole and chlorite are strongly enriched in Cr compared to epidote.

A simple Cr exchange in amphibole is not possible in tremolite-actinolite, and it must be combined with, for example, an Al exchange on the tetrahedrally coordinated site (Tschermak substitution) or with Na in M4 (glaucophane). Possible exchange-reactions with amphibole and epidote are therefore:

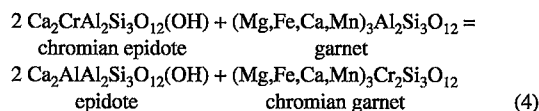


Complete ordering of ^{VI}Al in amphiboles into the M2 sites, and of Cr in epidote into M₁ sites, is possible, but as in chlorite, this intracrystalline cation-exchange is not well known. We therefore used the same X_{Cr} = Cr/(Cr + Oct) for epidote and amphibole (Fig. 11c).

In garnet and muscovite, the octahedrally coordinated sites are ideally occupied by two Al per formula unit, but there is no essential difference between ^{VI}Al sites in these minerals, and no preferential incorporation of Cr and Al on one of these sites has been reported. The exchange reactions are:



and



In contrast to garnet and muscovite, the Cr – Al substitution in epidote probably occurs in only one of

the three octahedral sites, M₁, as discussed above. It is therefore possible to compare the Cr/(Cr + ^{VI}Al) value in garnet and muscovite, respectively, with the Cr/(Cr + Al_{M1}) value in epidote (Fig. 11d). In this case, we see a preferred partitioning of Cr into epidote. If we were to use as X_{Cr} the same value as in Figure 11c (*i.e.*, not distinguishing between the different sites), all points would move near the line for $K_{Ex} = 1$.

We interpret the scatter of the data for distribution of Cr as a sign of disequilibrium, *i.e.*, the minerals crystallized over a range of P–T conditions, or the minerals did not achieve their complete chemical equilibrium because of the low mobility of Cr. It is impossible to distinguish between these two possibilities, and probably both are responsible. Texturally, no strong evidence of disequilibrium exists, though phengite (Fig. 7) probably crystallized over a range of P–T conditions, and chlorite shows reaction textures with epidote and amphibole. This large scatter of the data does not allow us to derive values for the distribution coefficient K_{Ex} . However, they indicate that among the investigated silicate minerals, epidote generally shows an enrichment in Cr. The enrichment is rather marked compared to that in chlorite and amphibole, less so compared to that in garnet, and similar to that in muscovite. The order of Cr enrichment (epidote = muscovite > garnet, chlorite, amphibole) is not the same as the one predicted by Burns (1970) on the basis of crystal-field stabilization energy (chlorite > garnet > epidote > tremolite > mica), but we emphasize that this question of “preferred enrichment” strongly depends on the formulation of the distribution coefficient.

Mobility of chromium during metamorphism

In the Nevado-Filábride metacarbonates, the original distribution of detrital grains of chromite is reflected in the concentration of chromian minerals in well-defined layers and an irregular distribution within these. The preservation of this sedimentary pattern suggests limited mobility of Cr during later metamorphic processes. During metamorphic recrystallization, Cr transport was limited to very short distances (< 1 mm) between chromite and crystallizing silicate phases, as reflected by heterogeneous distribution of Cr in large grains of epidote.

Treloar (1987a) also considered Cr immobility during metamorphism to be the reason for the Cr content and distribution of chromian minerals in the Outokumpu metasediments. In a study of the mineralization processes of metamorphic chromian beryl (emerald), Grundmann & Morteani (1989) also described the relatively low mobility of Cr (compared to Fe, Mg and Mn), even in the presence of a fluid phase. Tracy (1991), however, described chromian muscovite in veins and in the matrix of a calcite-dolomite marble, and related it to a fluid trans-

porting Cr from an unknown source. The higher mobility of Cr in this case is probably due to the large amount of fluid present and to its chemical composition. We agree with Treloar (1987a), who made a clear distinction between Cr immobility during metamorphism and its high mobility in later hydrothermal fluids. This is further supported by the study of Ottaway *et al.* (1994) on the hydrothermal formation of emerald from Colombia. They documented the mobility of Cr in H₂S-bearing fluids at low temperatures, approximately 300°C.

Interpretation of the high Zn content in chromian spinel inclusions

Zn-rich chromite is relatively scarce in nature and thus has received considerable attention in mineralogical literature (Bernier 1990, Béziat & Monchoux 1991, Mogessie *et al.* 1988, Pan & Fleet 1991). Some authors explain Zn enrichment as a primary magmatic feature of spinel (*e.g.*, Lamberg & Peltonen 1991, Wagner & Velde 1985), whereas in other cases metasomatic and hydrothermal processes are suggested (*e.g.*, Treloar 1987a, Wylie *et al.* 1987).

Some of the spinel inclusions in the Cr-rich minerals studied are very rich in Zn; we attribute this to the progressive removal of Cr, Fe, and Al from the original grains during metamorphism, and their simultaneous passive enrichment in Zn. This mechanism is easily understandable if one takes into account that silicate phases containing chromite inclusions (epidote, muscovite, amphibole, and chlorite) can easily accept Cr, Fe, and Al into their crystallographic structure. In contrast, Zn does not enter any of these minerals because of its different crystallochemical behavior. Zn²⁺ shows a strong preference for those minerals where tetrahedrally coordinated sites are occupied by divalent cations (Stoddard 1979) and especially for spinel (Marshall & Dollase 1984, Bruckmann-Bencke *et al.* 1988). Therefore both distribution coefficients for spinel and a variety of silicates (K_D and K_{Ex}) for Zn are $\gg 1$ (see Table 2 in Johnson 1994). In epidote, chlorite, muscovite, and amphibole, the tetrahedrally coordinated sites are occupied by Si⁴⁺ and Al³⁺ only, and Zn content is below the detection limit. This results in the passive relative enrichment of Zn in spinel compared to other cations. Since Mg also is accepted by all chromian minerals except epidote (which has only trace amounts of Mg; see Table 2), the low Mg content in inclusions of spinel in the epidote would seem to be a primary feature and not the result of metamorphism. An analogous process was reported by Gil Ibarguchi *et al.* (1991) to explain the enrichment of Cr in primary chromian spinel, transformed into chromite during metamorphism. No references exist on passive enrichment of Zn in chromite; nevertheless, Mogessie *et al.* (1988) described premetamorphic inclusions of chromite (with up to

2.52 wt.% ZnO) in uvarovitic garnet, and Zn-free chromite with the same origin in the matrix of a metacarbonate rock, which, in our opinion, can be interpreted in the same manner.

ACKNOWLEDGEMENTS

This study was supported by grants from Ministerio de Educación y Ciencia (Spain) and Deutscher Akademischer Austauschdienst (Germany) (Acciones Integradas) and by the Junta de Andalucía (Grupo de investigación 4019). We thank F. Galbert (Technische Universität Berlin, ZELMI), M.A. Hidalgo and I. Guerra (Servicios Técnicos, Univ. Granada) for their help with the electron microprobe and SEM analyses. We also thank C. Feixas and J.M. Alonso for their help in field work, J. Connolly, V. Trommsdorff and F. Bea for their revision of an earlier version of the manuscript, and C. Laurin for the English text. The paper was substantially improved as a result of the critical comments of two anonymous reviewers, M.R. St-Onge and R.F. Martin.

REFERENCES

- BAILEY, S.W. (1988): Chlorites: structures and crystal chemistry. In *Hydrous Phyllosilicates (Exclusive of Micas)* (S.W. Bailey, ed.). *Rev. Mineral.* **19**, 347-403.
- BERNIER, L.R. (1990): Vanadiferous zincian-chromian hercynite in a metamorphosed basalt-hosted alteration zone, Atik Lake, Manitoba. *Can. Mineral.* **28**, 37-50.
- BERNOULLI, D. & WINKLER, W. (1990): Heavy mineral assemblages from Upper Cretaceous South- and Austroalpine flysch sequences (northern Italy and southern Switzerland): source terranes and palaeotectonic implications. *Eclogae Geol. Helv.* **93**, 287-310.
- BERTOLANI, M., FIORI, S. & LOSCHI GHITTONI, A.G. (1991): Calc-silicate marbles in mafic rocks of the deep crust near Balmuccia (Ivrea-Zone). *Neues Jahrb. Mineral., Monatsh.* **6**, 241-252.
- BÉZIAT, D. & MONCHOUX, P. (1991): Les spinelles chromo-zincifères du district aurifère de Salsigne (Montagne Noire, France). *Eur. J. Mineral.* **3**, 957-969.
- BRUCKMANN-BENKE, P., CHATTERJEE, N.D. & AKSYUK, A.M. (1988): Thermodynamic properties of Zn(Al,Cr)₂O₄ spinels at high temperatures and pressures. *Contrib. Mineral. Petrol.* **98**, 91-96.
- BURNS, R.G. (1970): *Mineralogical Applications of Crystal Field Theory*. Cambridge University Press, London, U.K.
- & STRENS, R.G.J. (1967): Structural interpretation of the polarized absorption spectra of Al-Fe-Mn-Cr epidotes. *Mineral. Mag.* **36**, 204-226.
- BURNS, V.M. & BURNS, R.G. (1975): Mineralogy of chromium. *Geochim. Cosmochim. Acta* **39**, 903-910.

- CÁMARA, F. & GÓMEZ-PUGNAIRE, M.T. (1993): New data on the highest pressure and the PT-path of the Nevado-Filábride metabasites (SE Spain). *Terra* **5**, 400 (abstr.).
- CASTELLI, D. (1991): Eclogitic metamorphism in carbonate rocks: the example of impure marbles from the Sesia-Lanzo Zone, Italian Western Alps. *J. metamorph. Geol.* **9**, 61-77.
- CORTESOGNO, L., LUCCHETTI, G. & MASSA, B. (1981): Rocce of carbonato e marmi a silicati nel massiccio di Voltri: origine e significato, chimismo dei minerali ed equilibri paragenetici. *Rendi. Soc. Ital. Mineral. Petrol.* **37**, 481-507.
- DE JONG, K. & BAKKER, H.E. (1991): The Mulhacén and Alpujarride Complex in the eastern Sierra de los Filabres, SE Spain: lithostratigraphy. *Geol. Mijnbouw* **70**, 93-103.
- DEER, W.A., HOWIE, R.A. & ZUSSMAN, J. (1986): *Rock-Forming Minerals. 1B. Disilicates and Ring Silicates*. Longman, London, U.K.
- DOLLASE, W.A. (1971): Refinement of the crystal structures of epidote, allanite and hancockite. *Am. Mineral.* **56**, 447-464.
- _____ (1973): Mössbauer spectra and iron distribution in the epidote-group minerals. *Z. Kristallogr.* **138** (Buerger Festband), 41-63.
- EGELER, C.G. & SIMON, O.J. (1969): Orogenic evolution of the Betic Zone (Betic Cordilleras, Spain), with emphasis on the nappe structures. *Geol. Mijnbouw* **48**, 296-305.
- FERRY, J.M. (1976): Metamorphism of calcareous sediments in the Waterville-Vassalboro area, south-central Maine: mineral reactions and graphical analysis. *Am. J. Sci.* **276**, 841-882.
- FRANZ, G. & SELVERSTONE, J. (1992): An empirical phase diagram for the clinzoisite-zoisite transformation in the system $\text{Ca}_2\text{Al}_3\text{Si}_3\text{O}_{12}(\text{OH}) - \text{Ca}_2\text{Al}_2\text{Fe}^{3+}\text{Si}_3\text{O}_{12}(\text{OH})$. *Am. Mineral.* **77**, 631-642.
- _____ & SPEAR, F.S. (1983): High pressure metamorphism of siliceous dolomites from the central Tauern Window, Austria. *Am. J. Sci.* **283A**, 396-413.
- GABE, E.J., PORTHEINE, J.C. & WHITLOW, S.H. (1973): A reinvestigation of the epidote structure: confirmation of the iron location. *Am. Mineral.* **58**, 218-223.
- GARVER, J.I. & ROYCE, P.R. (1993): Chromium and nickel in shale of the foreland deposits of the Ordovician Taconic orogeny: using shale as a provenance indicator for ultramafic rocks. *Geol. Soc. Am., Abstr Programs* **25**(2), 17.
- GIL IBARGUCHI, J.I., MENDIA, M. & GIRARDEAU, J. (1991): Mg- and Cr-rich staurolite and Cr-rich kyanite in high-pressure ultrabasic rocks (Cabo Ortegal, northwestern Spain). *Am. Mineral.* **76**, 501-511.
- GÓMEZ-PUGNAIRE, M.T. (1979): Some considerations on the highest temperature reached in the outcropping rocks of the Nevado-Filábride Complex in the Sierra de Baza area during the Alpine metamorphism. *Neues Jahrb. Mineral. Abh.* **135**, 75-87.
- _____ (1981): Evolución del metamorfismo alpino en el Complejo Nevado-Filábride de la Sierra de Baza (Cordilleras Béticas, España). *Tecniterrae* **4**, 1-130.
- _____ & CÁMARA, F. (1990): La asociación de alta presión distena + talco + fengita coexistente con escapolita en metapelitas de origen evaporítico (Complejo Nevado-Filábride, Cordilleras Béticas). *Rev. Soc. Geol. España* **3**, 373-384.
- _____, CHACÓN, J., MITROFANOV, F. & TIMOFEEV, V. (1982): First report on pre-Cambrian rocks in the graphite-bearing series of the Nevado-Filábride Complex (Betic Cordilleras, Spain). *Neues Jahrb. Geol. Paläont., Monatsh.* **3**, 176-180.
- _____ & FERNÁNDEZ-SOLER, J.M. (1987): High-pressure metamorphism in metabasites from the Betic Cordilleras (S. E. Spain) and its evolution during the Alpine orogeny. *Contrib. Mineral. Petrol.* **95**, 231-244.
- _____, FONTBOTÉ, J.M. & SASSI, F.P. (1981): On the occurrence of a metaconglomerate in the Sierra de Baza (Nevado-Filábride Complex, Betic Cordilleras, Spain). *Neues Jahrb. Geol. Paläont., Monatsh.* **7**, 405-418.
- _____, FRANZ, G. & LÓPEZ SÁNCHEZ-VIZCAÍNO, V. (1994): Retrograde formation of NaCl-scapolite in high pressure metaevaporites from the Cordilleras Béticas (Spain). *Contrib. Mineral. Petrol.* **116**, 448-461.
- GRAPES, R.H. (1981): Chromian epidote and zoisite in kyanite amphibolite, Southern Alps, New Zealand. *Am. Mineral.* **66**, 974-975.
- GRUNDMANN, G. & MORTEANI, G. (1989): Emerald mineralization during regional metamorphism: the Habachtal (Austria) and Leydsdorp (Transvaal, South Africa) deposits. *Econ. Geol.* **84**, 1835-1849.
- HOSCHECK, G. (1980): Phase relations of a simplified marly rock system with application to the Western Hohe Tauern (Austria). *Contrib. Mineral. Petrol.* **73**, 53-68.
- JOHNSON, C.A. (1994): Partitioning of zinc among common ferromagnesian minerals and implications for hydrothermal mobilization. *Can. Mineral.* **32**, 121-132.
- KERRICH, R., FYFE, W.S., BARNETT, R.L., BLAIR, B.B. & WILLMORE, L.M. (1987): Corundum, Cr-muscovite rocks at O'Briens, Zimbabwe: the conjunction of hydrothermal desilicification and LIL-element enrichment - geochemical and isotopic evidence. *Contrib. Mineral. Petrol.* **95**, 481-498.

- LAFUSTE, M.J. & PAVILLON, M.J. (1976): Mise en évidence d'Eifélien daté au sein des terrains métamorphiques des zones internes des Cordillères Bétiques. Intérêt de ce nouveau repère stratigraphique. *C.R. Acad. Sci. Paris* **283**, sér. D, 1015-1018.
- LAIRD, J. (1988): Chlorites: metamorphic petrology. In *Hydrous Phyllosilicates (Exclusive of Micas)* (S.W. Bailey, ed.). *Rev. Mineral.* **19**, 405-453.
- LAMBERG, P. & PELTONEN, P. (1991): Chromian spinels in barren and fertile (Ni-Cu) Svecofennian 1.9 Ga ultramafic intrusions. *Terra* **3**(1), 111 (abstr.).
- LÓPEZ SÁNCHEZ-VIZCAÍNO, V.A. (1994): *Evolucion petrologica y geoquímica de las rocas carbonáticas y litologías asociadas en el área de Macael-Cóbdar (Almería), Complejo Nevado-Filábride, Cordilleras Béticas, SE España*. Tesis doctoral, Universidad de Granada, Granada, Spain.
- MARSHALL, C.P. & DOLLASE, W.A. (1984): Cation arrangement in iron-zinc-chromium spinel oxides. *Am. Mineral.* **69**, 928-936.
- MARTÍN-RAMOS, J.D. & RODRÍGUEZ-GALLEGO, M. (1982): Chromian mica from Sierra Nevada, Spain. *Mineral. Mag.* **46**, 269-272.
- _____, _____ & BURGOS, J.C. (1979): Sobre una mica crómica de Sierra Nevada. *Soc. Esp. Mineral.* **1**, 93-102.
- MASSONNE, H.-J. & SCHREYER, W. (1987): Phengite geobarometry based on the limiting assemblage with K-feldspar, phlogopite, and quartz. *Contrib. Mineral. Petrol.* **96**, 212-224.
- MAX, M.D., TRELOAR, P.J., WINCHESTER, J.A. & OPPENHEIM, M.J. (1983): Cr mica from the Precambrian Erris Complex, NW Mayo, Ireland. *Mineral. Mag.* **47**, 359-364.
- McKAY, G.A. (1989): Partitioning of rare earth elements between major silicate minerals and basaltic melts. In *Geochemistry and Mineralogy of the Rare Earth Elements* (B.R. Lipin & G.A. McKay, eds.). *Rev. Mineral.* **21**, 45-77.
- MOGESSIE, A., PURTSCHHELLER, F. & TESSADRI, R. (1988): Chromite and chrome spinel occurrences from meta-carbonates of the Oetzal-Stubai Complex (northern Tyrol, Austria). *Mineral. Mag.* **52**, 229-236.
- NIJHUIS, H.J. (1964): *Plurifacial Alpine Metamorphism in the Southeastern Sierra de los Filabres South of Lubrin, SE Spain*. Thesis, Amsterdam Univ., Amsterdam, The Netherlands.
- OTTAWAY, T.L., WICKS, F.J., BRYNDZIA, L.T., KYSER, T.K. & SPOONER, E.T.C. (1994): Formation of the Muzo hydrothermal emerald deposit in Colombia. *Nature* **369**, 552-554.
- PAN, YUANMING & FLEET, M.E. (1989): Cr-rich calc-silicates from the Hemlo area, Ontario. *Can. Mineral.* **27**, 565-577.
- _____, _____ (1991): Barian feldspar and barian-chromian muscovite from the Hemlo area, Ontario. *Can. Mineral.* **29**, 481-498.
- PAPIKE, J., CAMERON, K.L. & BALDWIN, K. (1974): Amphiboles and pyroxenes: characterization of other than quadrilateral components and estimates of ferric iron from microprobe data. *Geol. Soc. Am., Abstr. Programs* **6**, 1053.
- PRIEM, H.N.A., BOELRIJK, N.A.I.M., HEBEDA, E.H. & VERSCHURE, R.H. (1966): Isotopic age determinations on tourmaline granite-gneisses and a metagranite in the eastern Betic Cordilleras (southeastern Sierra de los Filabres), SE Spain. *Geol. Mijnbouw* **45**, 184-187.
- PUGA, E. & DÍAZ DE FEDERICO, A. (1978): Metamorfismo polifásico y deformaciones alpinas en el Complejo de Sierra Nevada (Cordillera Bética). Implicaciones geodinámicas. *Reunión Geol. Cord. Bética y Mar de Alborán (Granada)*, 79-112.
- _____, REYES, E., CABALLERO, E., TENDERO, J.A., NIETO, J.M. & DÍAZ DE FEDERICO, A. (1992): Caracterización preliminar del ambiente de génesis de la secuencia sedimentaria de las ofiolitas Béticas y de la Formación Soportujar mediante isótopos de oxígeno y carbono. *III Congr. Geol. España I*, 362-366.
- SPEAR, F.S. (1993): Metamorphic phase equilibria and pressure - temperature - time paths. *Mineral. Soc. Am., Monogr.* **1**.
- STODDARD, E.F. (1979): Zinc-rich hercynite in high-grade metamorphic rocks: a product of dehydration of staurolite. *Am. Mineral.* **64**, 736-741.
- THOMPSON, J.B., JR. (1982): Composition space: an algebraic and geometric approach. In *Characterization of Metamorphism through Mineral Equilibria* (J.M. Ferry, ed.). *Rev. Mineral.* **10**, 1-31.
- TRACY, R.J. (1991): Ba-rich micas from the Franklin Marble, Lime Crest and Sterling Hill, New Jersey. *Am. Mineral.* **76**, 1683-1693.
- TRELOAR, P.J. (1987a): The Cr-minerals of Outokumpu. Their chemistry and significance. *J. Petrol.* **28**, 867-886.
- _____, _____ (1987b): Chromian muscovites and epidotes from Outokumpu, Finland. *Mineral. Mag.* **51**, 593-599.
- UTTER, T. (1978): The origin of detrital chromites in the Klerksdorp Goldfield, Witwatersrand, South Africa. *Neues Jahrb. Mineral., Abh.* **133**, 191-209.

- VOET, H.W. (1967): *Geological Investigations in the Northern Sierra de los Filabres around Macael and C6bdar, South-Eastern Spain*. Thesis, Amsterdam Univ., Amsterdam, The Netherlands.
- WAGNER, C. & VELDE, D. (1985): Mineralogy of two peralkaline, arfvedsonite-bearing minettes. A new occurrence of zinc-rich chromite. *Bull. Minéral.* **108**, 173-187.
- WARD, C.M. (1984): Magnesium staurolite and green chromian staurolite from Fiordland, New Zealand. *Am. Mineral.* **69**, 531-540.
- WILSON, C. (1975): *Carbonate Facies in Geologic History*. Springer, Berlin, Germany.
- WINKLER, W. & BERNOULLI, D. (1986): Detrital high pressure/low temperature minerals in a Late Turonian flysch sequence of the eastern Alps (western Austria): implications for early Alpine tectonics. *Geology* **14**, 598-601.
- WOOD, B.J. & FRASER, D.G. (1977): *Elementary Thermodynamics for Geologists*. Oxford University Press, Oxford, U.K.
- WYLIE, A.G., CANDELA, P.A. & BURKE, T.M. (1987): Compositional zoning in unusual Zn-rich chromite from the Sykesville district of Maryland and its bearing on the origin of "ferritchromit". *Am. Mineral.* **72**, 413-422.

Received December 13, 1993, revised manuscript accepted July 27, 1994.